cancers

# Supplementary Material: The interaction between reactive peritoneal mesothelial cells and tumor cells via extracellular vesicles facilitates colorectal cancer dissemination

**Simona Serratì, Letizia Porcelli, Francesco Fragassi, Marianna Garofoli, Roberta Di Fonte, Livia Fucci, Rosa Maria Iacobazzi, Antonio Palazzo, Francesca Margheri, Grazia Cristiani, Anna Albano, Raffaele De Luca, Donato Francesco Altomare , Michele Simone and Amalia Azzariti**

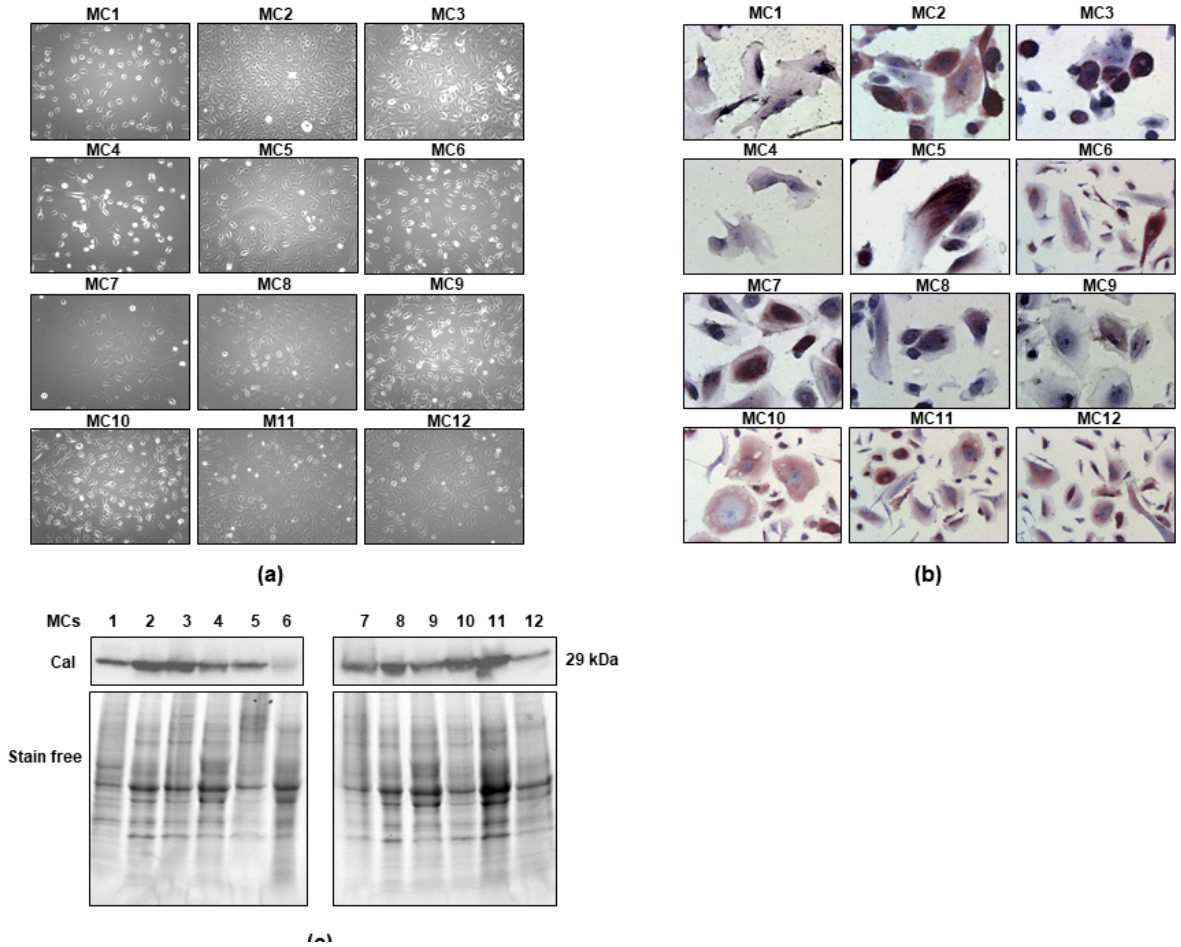


**Figure S1.** Characterization of the peritoneal mesothelial cell lines. **a**) Images of optical microscopy showing the morphology of the 12 MC cell lines isolated from the PLF of 12 colorectal cancer patients. **b**) Images showing the immunostaining of fixed MC cell lines with the anti-calretinin (Cal) antibody (red color) showing variable expression of the biomarker among the 12 cell lines. Counterstain of nuclei was done with Hematoxilin. (magnification x100). **c**) Western blot analysis of Cal protein expression in the 12 MC cell lines. Stain free detection iss used as loading control.

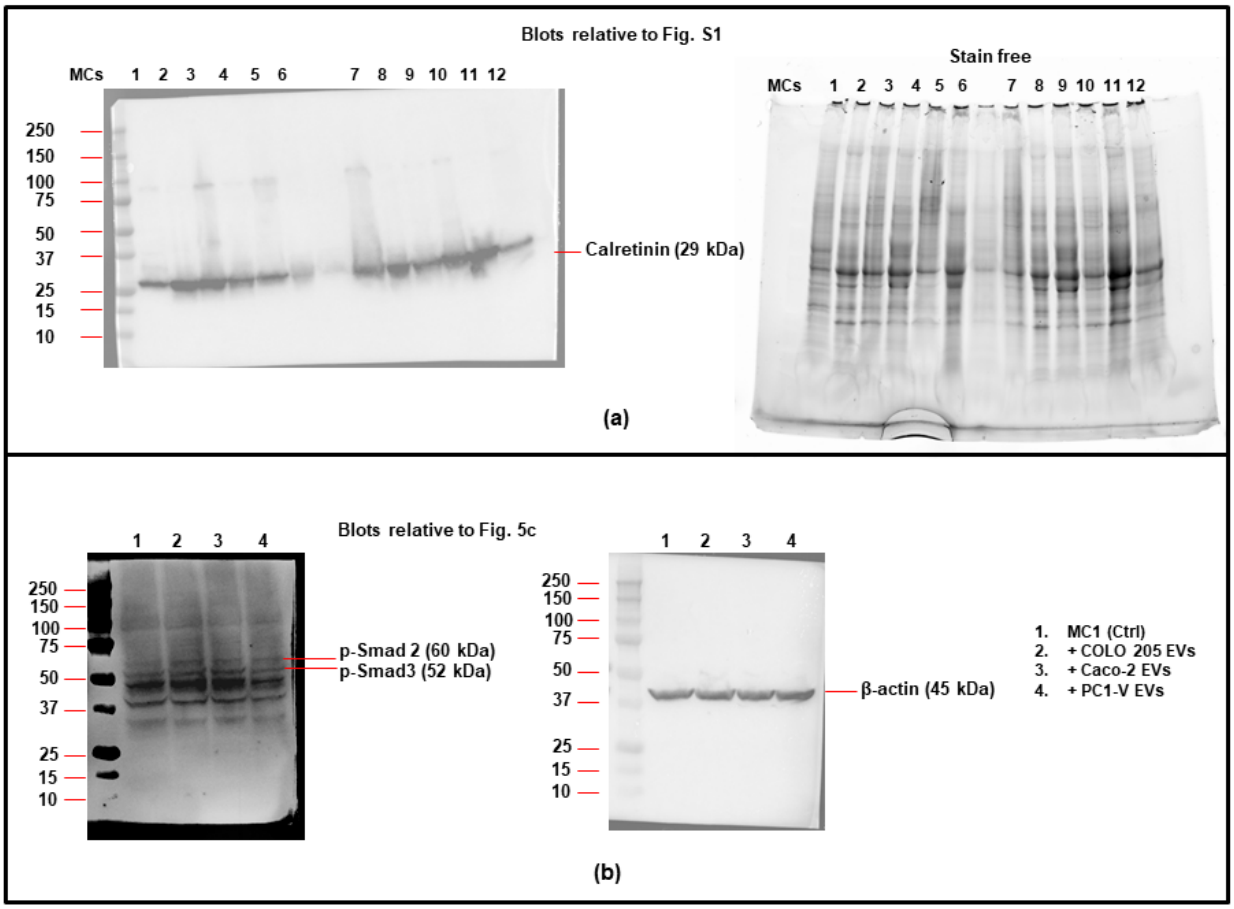


**Figure S2**. Whole blot related to Figure S1 and Figure 5c. Image**s** showing all the bands with all molecular weight markers on the Western Blot for Calretinin expression with relative complete stain-free gel (a), and whole blot for p-SMAD 2/3 expression with relative◎◎-Actin expression.

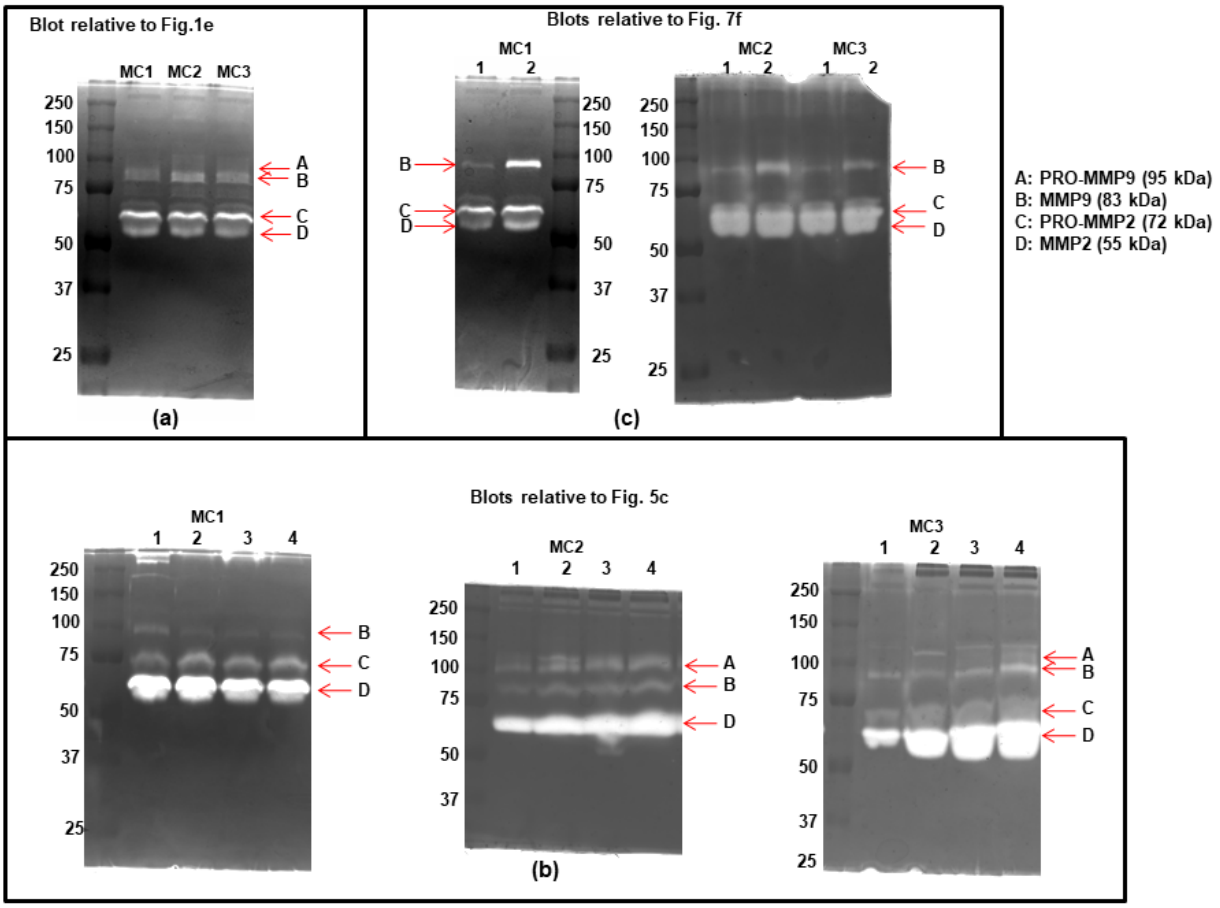


**Figure S3.** Whole gel related to gelatin zymography assay. Immages showing molecular weight markers relative to gelatin zymography rapresented in Figure 1 (a), Figure 5c (b) and Figure 7f (c).

| Cell line | In vitro | | | In vivo | | | | |
|---|---|---|---|---|---|---|---|---|
| | Growth pattern | Doubling time (h) | Cell morphology | sex | age | Original size of cell line | pathology | TNM stage |
| **PC1-V** | Adherent | 34 | Polygonal | M | 42 | Ascites | Peritoneal carcinosis from colon carcinoma | T4 |

**(a)**

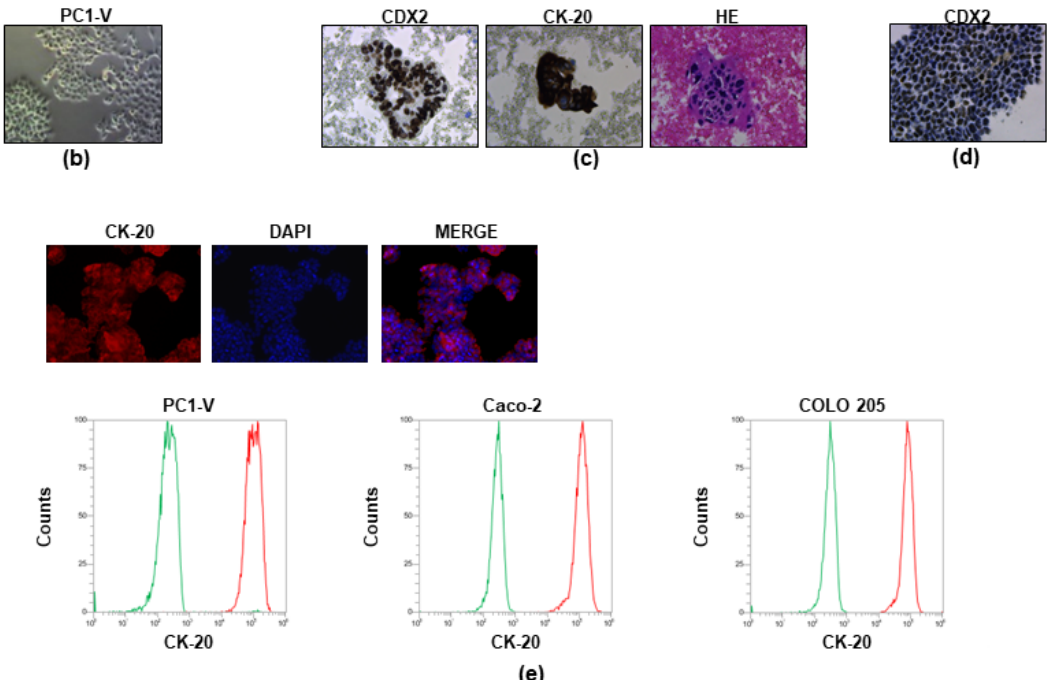


**Figure S4.** Establishment and characterization of primary cancer cell line PC1-V. **a**) In vitro and in vivo characteristics of PC1-V cells. **b**) Images of optical microscopy showing PC1-V cells displaying an epithelial-like morphology and an adherent growth. **c**) Images showing CDX2 and CK-20 positivity by immunoperoxidase staining and the HE staining of the patient cytological sample. D) CDX2 positivity of PC1-V cells by IHC. E) Images of fluorescence microscopy showing CK-20 positivity in PC1-V cells determined by IF, and FCM. The latter analysis shows the expression of CK-20 in comparison with COLO 205 and Caco-2 cell lines by FCS.

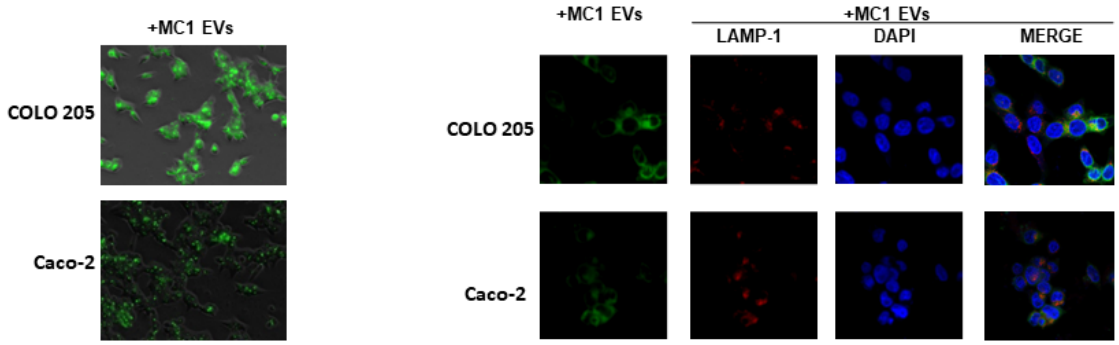


**Figure S5.** PKH67-MC1 EVs are internalized in tumor cells and colocalize with lysosome marker LAMP-1. Representative images of fluorescence and phase-contrast microscopy showing fluorescent PKH67-MC1 EVs (green) in Caco-2 and COLO 205 cell lines (magnification x400) and representative images of fluorescence confocal microscopy showing PKH67-MC1

EVs (green) uptake and colocalization with LAMP-1 (red) in Caco-2 and COLO 205 cell lines. Nuclei are counterstained with Dapi (blue) (magnification x100).

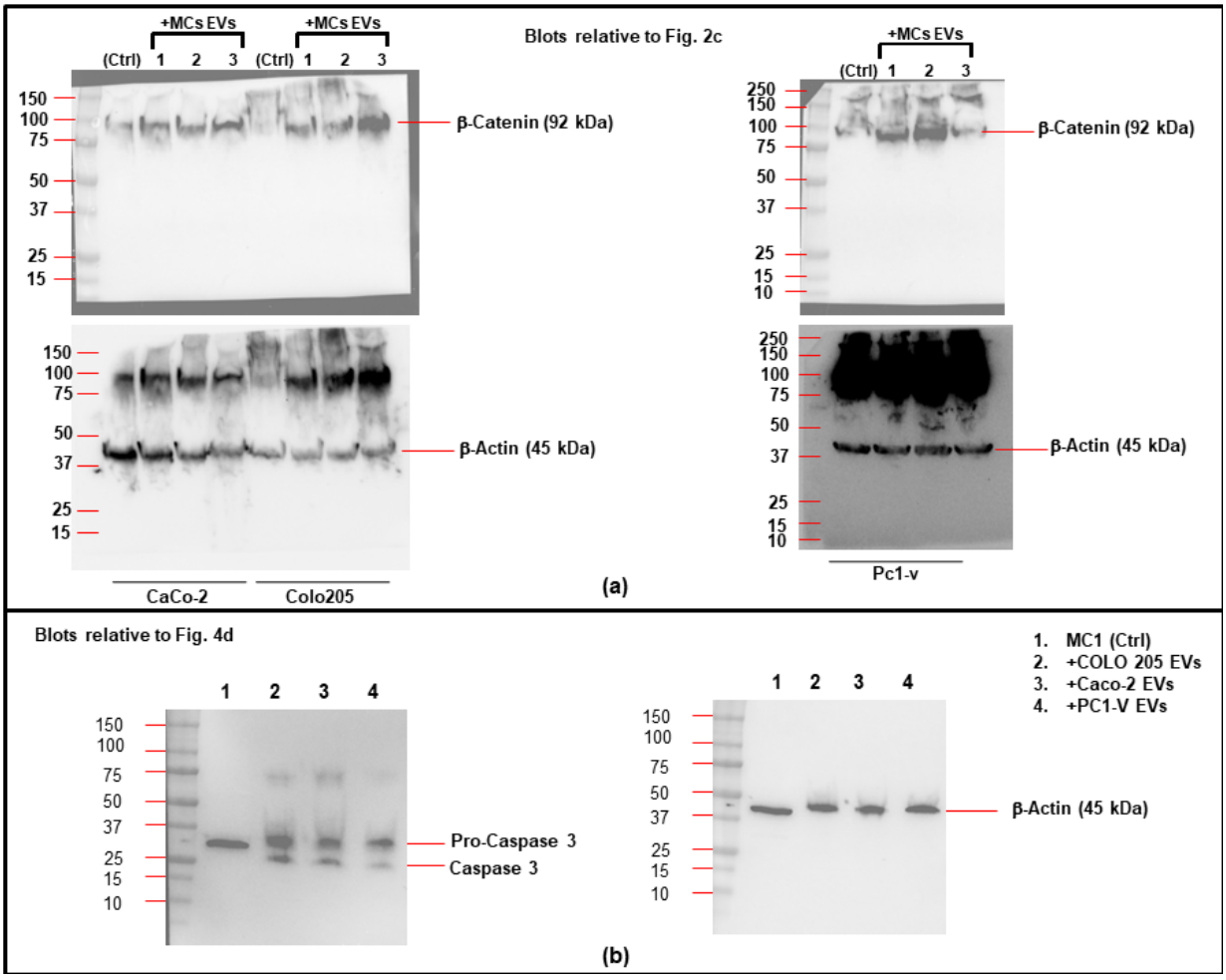


**Figure S6.** Whole blot related to Figure 2c and Figure 4d. Image**s** showing all the bands with all molecular weight markers on the Western Blot for ⊚-Catenin with relative ⊚-Actin expression (a), and whole blot for Caspase-3 expression with relative ⊚-Actin expression (**b**).

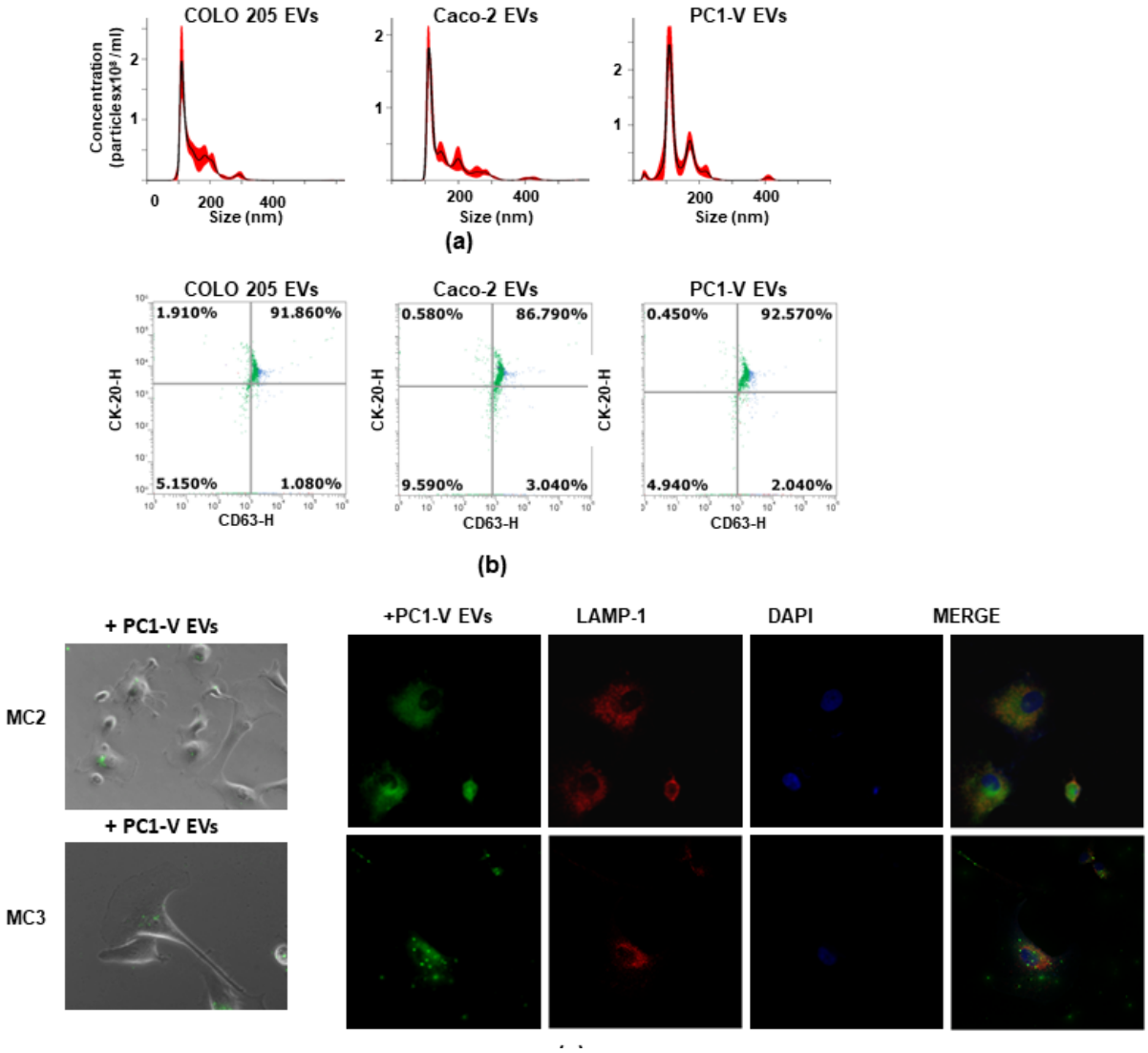


**Figure S7.** Internalization and characterization of tumor-EVs**. a)** Nanoparticle tracking analyses showing the concentration and the size of EVs released by tumor cell lines. **b**) Dot plots corresponding to the FCM analysis of EVs released by tumor cells (CK-20), showing that the majority of them are $CD63^+$ one. **c**) Representative images of fluorescence and phase-contrast microscopy showing fluorescent PKH67-PC1-V EVs (green) in MC2 and MC3 cell lines (magnification x400) and representative images of fluorescence confocal microscopy showing PKH67-PC1-V EVs (green) uptake and colocalization with LAMP-1 (red) in Caco-2 and COLO 205 cell lines. Nuclei are counterstained with Dapi (blue) (magnification x100).

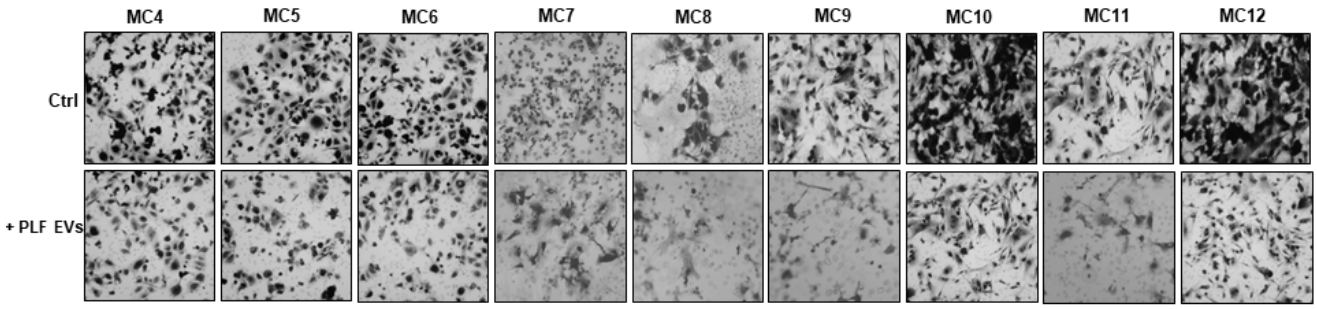

**Figure S8**. PLF EVs pool reduces mesothelial cells motility. Representative images of optical microscopy showing that PLF EVs pool isolated from the PLF of each patient reduces the motility of MC4-12 cell lines.

**Table S1.** Materials. Flow Cytometry (FCM), Immunohistochemistry (IHC), Immunofluorescence (IF), Western blot (WB).

| Product | Catalog n. | Company | Assay | Concentration of usage |
|---|---|---|---|---|
| anti-CD9-Super Bright 436 | 62-0098-42 | e-Biosciences, Thermo Fisher Scientific, Waltham, MA USA | FCM | 5 μL (0.25 μg)/test |
| anti-CD63-PE-Cyanine7 | 25-0639-42 | e-Biosciences, Thermo Fisher Scientific, Waltham, MA USA | FCM | 5 μL (0.25 μg)/test |
| anti-CD81- PerCP-eFluor 710 | 44-0819-42 | e-Biosciences, Thermo Fisher Scientific, Waltham, MA USA | FCM | 5 μL (0.25 μg)/test |
| anti-CD44-VioBlue | 130-113-337 | Miltenyi Biotec, Bergisch Gladbach, Germany | FCM | 2 μL /test |
| anti-CK-20-PE | ab209923 | Abcam, Cambridge, UK | FCM | 1/500 |
| anti-a-SMA | A5228 | Sigma-Aldrich, St. Louis, MO, USA | IF | 2 μg /ml |
| anti-Vimentin | V6630 | Sigma-Aldrich, St. Louis, MO, USA | IF | 1:500 |
| anti-Lamp-1 | #9091 | Cell Signaling Technology, Danvers, MA, USA | IF | 1:200 |
| anti-β-Actin | #3700 | Cell Signaling Technology, Danvers, MA, USA | WB | 1:1000 |
| anti-⍵-Catenin | #8480 | Cell Signaling Technology, Danvers, MA, USA | WB | 1:1000 |
| anti- p-Smad2/3 | #8828 | Cell Signaling Technology, Danvers, MA, USA | WB | 1:1000 |
| anti-CK-20 | MA5-31979 | Invitrogen, ThermoFisher Scientific, Waltham, MA USA | WB, IHC | 1:1000, 1:200 |
| anti-Calretinin | PA5-16681 | Invitrogen, ThermoFisher Scientific, Waltham, MA USA | WB | 1:500 |
| anti-uPAR (R-4) | MON-R-4-02 | Invitrogen, ThermoFisher Scientific, Waltham, MA USA | WB | 1:500 |
| anti-CDX2 | PA0375 | Novocastra, Leica Biosystems, Wetzlar, Germany | IHC | According the manufacturer instructions. |
| anti-Caspase 3 | sc-7272 | Santa Cruz Biotechnology, Inc | WB | 1:500 |
| Alexa Fluor™ 568 goat anti-mouse IgG | A11004 | Molecular Probes, Life Thecnologies, ThermoFisher Scientific, Waltham, MA USA | IF | 1:1000 |
| Alexa Fluor™ 488, Goat anti-Mouse IgG | A11001 | Molecular Probes, Life Thecnologies, ThermoFisher Scientific, Waltham, MA USA | IF | 1:1000 |
| Goat Anti-Mouse IgG (H + L)-HRP Conjugate | #1706516 | BIORAD, Hercules, CA, USA | WB | 1:2000 |
| Goat Anti-Rabbit IgG (H + L)-HRP Conjugate | #1706515 | BIORAD, Hercules, CA, USA | WB | 1:2000 |
| | | **Other materials** | | |
| SB complete staining buffer | SB-4401-42 | e-Biosciences, Thermo Fisher Scientific, Waltham, MA USA | FCS | 2 μL /test |
| Phalloidin-iFluor 555 | ab176756 | Abcam, Cambridge, UK | IF | 1:500 |

| | | | | |
|---|---|---|---|---|
| DAPI (4',6-Diamidino-2-Phenylindole, Dihydrochloride) | D1306 | Invitrogen, ThermoFisher Scientific, Waltham, MA USA | IF | 300 nM |
| Green Fluorescent Cell Linker | MIDI67-1KT | Sigma-Aldrich St. Louis, MO, USA | IF | According the manufacturer instructions. |
| FITC Annexin V Apoptosis Detection Kit I | 556547 | BD Pharmingen™, San Jose, CA, USA | FCM | According the manufacturer instructions. |
| Pantoprazolo | AIC n. 044465019 | SUN Pharma, Sun Pharmaceutical Industries Ltd. Goregaon, Mumbai, India | Functional studies. | 1.25 and 2.5 μg/mL |

**Table S2.** Intensity ratio of Western Blot images showing in Figures 2c, 4d, 5c, and densitometry readings and showing in S1c.

| **Fig. 2c** | **⚜-catenin normalized to ⚜-actin** | | | |
|---|---|---|---|---|
| | **Ctrl** | **1** | **2** | **3** |
| **CaCo-2** | 2758321 | 7242274 | 8653667 | 16913705 |
| **Colo205** | 1832862 | 12729893 | 12410528 | 28636569 |
| **PC1-V** | 3694842 | 6462198 | 12200514 | 3502585 |

| **Fig. 4d** | **Caspase-3 normalized to stain free loading sample** | | | |
|---|---|---|---|---|
| **MC1** | **1** | **2** | **3** | **4** |
| **Pro-caspase 3** | 2746633,0 | 2873901,0 | 2671387,0 | 1406835,0 |
| **Pro-caspase 3** | 2364687,0 | 1926893,0 | 1724544,0 | 1116577,0 |
| **Pro-caspase 3** | 1746053,0 | 1497555,0 | 1945360,0 | 1482869,0 |
| **Cleaved-caspase 3** | 0,0 | 1950548,0 | 1628676,0 | 1457912,0 |
| **Cleaved-caspase 3** | 0,0 | 705569,0 | 670084,0 | 350212,0 |
| **Cleaved-caspase 3** | 0,0 | 510012,0 | 860598,0 | 399062,0 |
| **Fig. 5c** | **p-Smad 2/3 normalized to ⚜-actin** | | | |
| | **1** | **2** | **3** | **4** |
| **MC1** | 650268 | 1010550 | 1034423 | 601284 |

| **Fig. S1c** | **Calretinin normalized to stain free loading sample** |
|---|---|
| **MC1** | 29929760 |
| **MC2** | 46105576 |
| **MC3** | 30430095 |
| **MC4** | 36015056 |
| **MC5** | 23936169 |
| **MC6** | 20235378 |
| **MC7** | 62560320 |
| **MC8** | 45822171 |
| **MC9** | 36938573 |
| **MC10** | 39728671 |
| **MC11** | 35155302 |
| **MC12** | 18000704 |

**Table S3.** Densitometry readings of the gelatine zymography bands showing in Figure S3.

| | Volume (Int) | | | |
|---|---|---|---|---|
| **Fig. 1e** | ***MC1*** | ***MC2*** | ***MC3*** | |
| PRO-MMP9 | 19562810 | 29291036 | 24691106 | |
| MMP9 | 16427924 | 24536384 | 18150410 | |
| PRO-MMP2 | 177001112 | 155704902 | 158612306 | |
| MMP2 | 118238424 | 101007572 | 86408920 | |
| | | | | |
| **Fig. 5c** | ***MC1 - 1*** | ***MC1 - 2*** | ***MC1 - 3*** | ***MC1 - 4*** |
| MMP9 | 24391872 | 8686700 | 9257616 | 6643020 |
| PRO-MMP2 | 46332176 | 85406320 | 75051604 | 93743856 |
| MMP2 | 708335036 | 713850852 | 591925624 | 571421832 |
| | | | | |
| **Fig. 5c** | ***MC2 - 1*** | ***MC2 - 2*** | ***MC2 - 3*** | ***MC2 - 4*** |
| MMP9 | 22999633 | 55709908 | 76030263 | 35807966 |
| PRO-MMP2 | 18996963 | 46943491 | 48648793 | 61235576 |
| MMP2 | 403678870 | 621366515 | 742713670 | 787844249 |
| | | | | |
| **Fig. 5c** | ***MC3 - 1*** | ***MC3 - 2*** | ***MC3 - 3*** | ***MC3 - 4*** |
| PRO-MMP9 | 807618 | 2615412 | 1454637 | 3783423 |
| MMP9 | 25042791 | 22703754 | 35798502 | 79788759 |
| PRO-MMP2 | 19690563 | 49007016 | 76343619 | 70492308 |
| MMP2 | 241223718 | 579251850 | 701774817 | 737940345 |
| | | | | |
| **Fig. 7f** | ***MC1 - 1*** | ***MC1 - 2*** | | |
| MMP9 | 13349760 | 130981260 | | |
| PRO-MMP2 | 138386052 | 176989788 | | |
| MMP2 | 70971804 | 147619704 | | |
| | | | | |
| **Fig. 7f** | ***MC2 - 1*** | ***MC2 - 2*** | ***MC3 - 1*** | ***MC3 - 2*** |
| MMP9 | 74021850 | 150233370 | 49366590 | 52628520 |
| PRO-MMP2 | 269053260 | 303433830 | 270572610 | 294616350 |
| MMP2 | 199226790 | 218666910 | 188038200 | 199434270 |